Emergency Vehicle Maneuvers and Control Laws for Automated Highway Systems

Charmaine Toy, Kevin Leung, Luis Alvarez, and Roberto Horowitz, *Senior Member, IEEE*

***Abstract*—The operation and transit of emergency vehicles on an automated highway system (AHS) designed under the control architecture proposed in the California Partners for Advanced Transit and Highways (PATH) program is described. The term emergency vehicles is used in a general sense to describe vehicles, such as police cars, ambulances, and tow trucks, that may service faults inside or outside the AHS. The transit of emergency vehicles requires intensive participation of the coordination layer, which directs the interactions of neighboring vehicles, and the link layer, which regulates traffic flow along stretches of highway. Various strategies for these two hierarchical layers that are needed to assign high-priority transit to emergency vehicles (EVs) on the AHS are described. These coordination and link layer maneuvers circulate vehicles around the EV in both free-flowing and stopped traffic.**

***Index Terms*—Discrete event systems, hierarchical control systems, traffic flow control, vehicle control.**

I. Introduction

THE automated highway system's (AHSs) capability to maintain high traffic flows is directly related to its ability to quickly recover from faults. Assuming, for example, that there is on average a breakdown per vehicle every 6000 miles and that a single-lane AHS has a maximum capacity of 6000 vehicles per hour, it is possible to expect one breakdown per hour in an AHS lane. Proper handling of certain faults within the AHS, such as stopped vehicles or accidents, requires emergency vehicle (EV) transit and service inside the AHS. Moreover, EVs may use the AHS to travel faster to a remote incident outside of the system.

This paper investigates the conditions to achieve EV access and transit using the hierarchical control systems AHS architecture proposed in [1] and [2] that partitions the design of the AHS into five layers: network, link, coordination, regulation, and physical. This paper focuses upon research pertinent to the coordination and link layers. The coordination layer directs the interactions of neighboring vehicles, and includes both communication and decision logic for individual vehicles. The link layer regulates traffic flow along stretches of highway and does not control individual vehicles.

Manuscript received October 25, 1999; revised May 3, 2002. This work was supported by the California Partners for Automated Transit and Highways (PATH) under Project MOU-311. The contents of this paper reflect the views of the authors and do not necessarily reflect the official policies of California PATH. The paper does not constitute a standard, specification, or regulation.

C. Toy is with DiCon Fiberoptics, Richmond, CA 94804 USA.

K. Leung is with Phaethon Communications, Freemont, CA 94538 USA.

L. Alvarez is with the Universidad Nacional Autónoma de México, DF 04520 México.

R. Horowitz is with the University of California at Berkeley, Berkeley, CA 94720-1740 USA (e-mail: horowitz@me.berkeley.edu).

Publisher Item Identifier 10.1109/TITS.2002.801422.

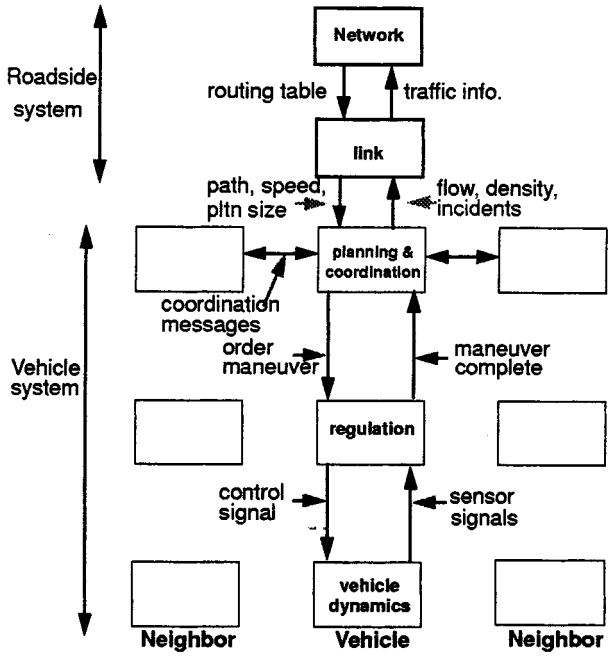

Fig. 1. California Partners for Advanced Transit and Highways (PATH) hierarchical control architecture.

The link layer control laws and coordination-layer maneuvers presented in this paper address two design objectives.

1) **To ensure rapid EV transit within the AHS:** The EV travels to an incident inside or outside of the system. Traffic flow conditions are relatively close to nominal.
2) **To promote EV transit through stopped AHS traffic:** Traffic flow may be stopped due to an accident or other fault. Maneuvers are required to move other vehicles out of the EV's path and to transport the EV to the incident site.

Both scenarios require EVs to have higher transit priority than other vehicles in the AHS, which requires changes to the normal operating modes of the AHS. Normal vehicle maneuvers may be interrupted for control commands to make way for the EV. Relaxation of certain AHS parameters, such as comfortable maximum deceleration/acceleration, may also be possible. These changes result in *degraded mode* operation of the AHS in a neighborhood of the EV (see [3] and [4] for additional description of the degraded modes of operation). The design for EV transit on an AHS makes the following assumptions.

1) **There are two or more AHS lanes:** The lane in which the EV does not travel is used to circulate vehicles around the EV. In this paper, all designs and control laws assume that highways have two lanes everywhere.

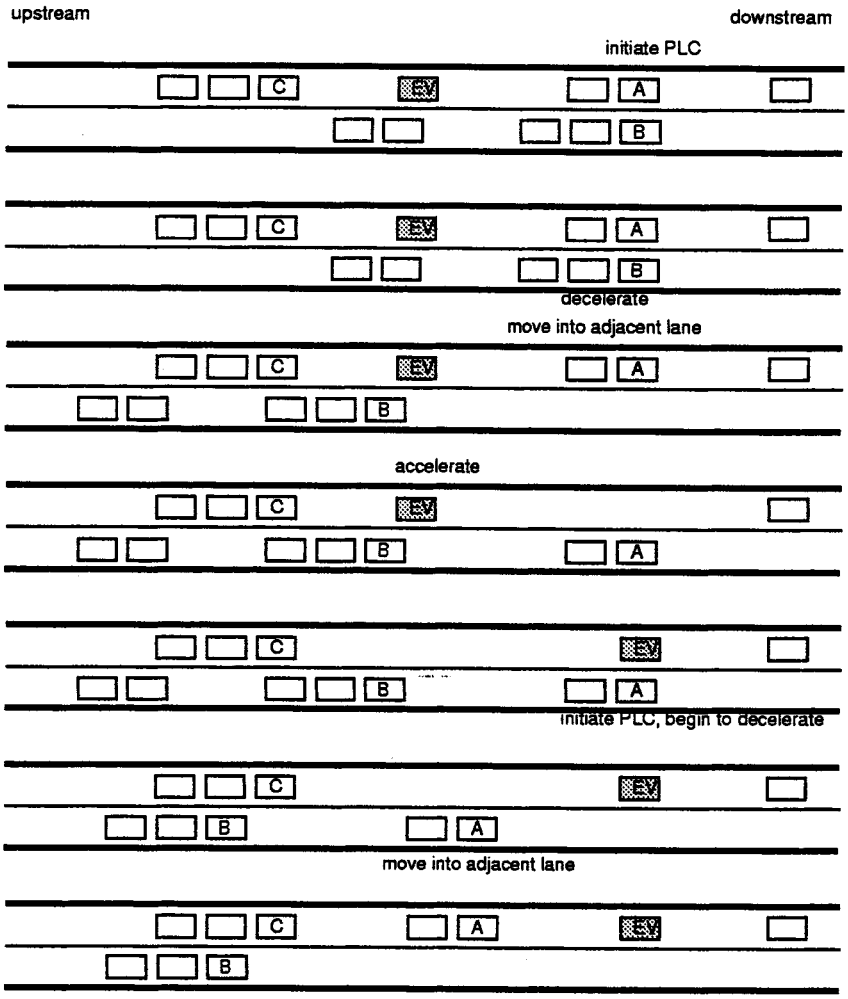

Fig. 2. Vortex maneuver.

2) **There is no dedicated shoulder for the EV:** The EV travels through normal automated lanes. One of the purposes of AHS design is to increase traffic capacity while using less roadway space. The rationale arises from the assumption that space used for a shoulder could be utilized for a highway lane instead.
3) **All vehicles on the AHS are fully automated:** All AHS vehicles are able to interpret commands to assign the EV high priority transit.

II. PATH AHS ARCHITECTURE

In the AHS control architecture proposed in [1] and [2] traffic is organized into platoons of closely spaced vehicles. The use of this strategy achieves the objective of increasing highway capacity and safety. Platoons have large interplatoon distances (i.e., 40 m) and small intraplatoon spacings (i.e., 2 m). The first vehicle of a platoon is called the leader, while all other vehicles in the platoon are called followers; a single vehicle by itself in a platoon is denoted a free-agent. The design of the AHS architecture shown in Fig. 1 consists of five hierarchical layers: network, link, coordination, regulation, and physical [1], [2]. The first two layers are roadside control systems, and the latter three reside on each vehicle. The purpose of the hierarchical control structure is to partition the complex problem of controlling an AHS and all its vehicles into several control problems which can be separately designed. Each hierarchical layer provides a reference model to its adjacent control layers. Each hierarchical layer is described below.

One network-layer controller exists for the entire automated highway network. It is responsible for assigning a specific route to the vehicles based on the vehicle destinations. The network layer controller minimizes the travel time of vehicles by choosing optimal vehicle routes. Control is exerted by specifying activities at highway junctions to the link-layer controller.

An AHS network is divided into links, or sections, that can vary from hundreds of meters to a few kilometers. A single link-layer controller controls several links. The link layer does not identify individual vehicles, but rather specifies velocities, platoon size, and proportions of activities for a particular vehicle destination or type on each link. Roadside sensors provide density information for the different types of vehicles on each link. Control commands from the link layer are passed to the coordination layer [5]–[7].

The coordination layer determines what maneuvers to perform, manages intervehicle communications, and coordinates the movement of the vehicle with neighboring cars. The choice

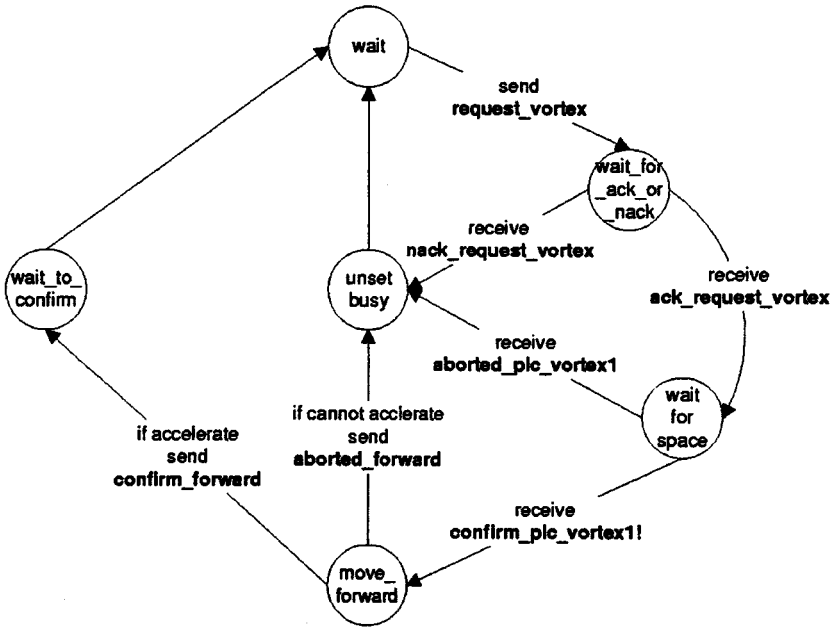

Fig. 3. Vortex initiator's (EV) FSM.

of maneuvers and when to execute them depend on safety, the vehicle's route, commands from the link layer, and local traffic conditions [8], [9], [5], and [10]. The vehicle speed transmitted by the link layer to the coordination layer is passed directly to the regulation-layer controllers and is not directly utilized by the coordination layer. The proportion of activities broadcasted to each vehicle's coordination layer determines a probability for maneuver initiation (e.g., merge, split, or change lane). At present, each vehicle's probability of maneuver execution is independent of its local state.

The regulation layer receives commands from the coordination layer and executes the chosen maneuvers. It is essentially a set of continuous-time feedback-based controllers [8], [10].

The lowest hierarchical level is the physical layer, which pertains to the vehicle's actuators and sensors. It receives steering, throttle, and brake actuator commands from the regulation layer and returns information such as vehicle speed, acceleration, and engine state.

For safety reasons, vehicle control is exerted with the lower hierarchical-level commands taking greater priority over ones from higher levels. Conversely, optimization of overall traffic flow is exerted from the top down. Commands from the roadside link-layer controller, such as proportions of vehicles changing lane, are transmitted to each vehicle's on-board coordination layer. The coordination-layer controller then interprets the control command without violating the safety conditions imposed at the lower hierarchical levels. For example, a change-lane maneuver will not be successful if the vehicles in the destination lane are unable to guarantee safe space.

III. Coordination-Layer Design

For the coordination layer, three EV maneuvers: the vortex, part-and-go, and zig-zag; were developed to facilitate EV transit on the AHS. The decision logic of these maneuvers is modeled with finite state machines (FSM). Coordination-layer design is specific to the PATH architecture, and extensive work has been devoted to the development of coordination-layer maneuvers [8], [11], [12]. The FSMs developed for all maneuvers, except the Vortex, were verified using the software package COSPAN [13], [14]. The Vortex FSMs were verified using UPPAAL [15].

A. Vortex Maneuver

The objective of the vortex maneuver is to circulate traffic around the EV to allow it to travel faster than the normal traffic flow and causing minimal disturbance to the freely flowing AHS. The goal is to assist an EVs (e.g., ambulance) transit within the AHS so that it can reach its destination as quickly as possible. The name of the maneuver was adopted because its execution produces a traffic-flow pattern that resembles a vortex in a fluid. Fig. 2 illustrates the general operation of the vortex maneuver, which employs the platoon-lane-change maneuver (PLC). The PLC maneuver permits a full platoon to change lanes, as opposed to the normal lane-change maneuver that only allows a single vehicle to change lanes.

When the EV initiates the vortex maneuver upon entering the AHS, it travels as fast ($V_{\max}^{EV}$) as the link layer allows if no traffic is ahead. When it encounters a front platoon (first responder, marked A in Fig. 2), it slows to the normal traffic speed and requests a PLC maneuver. A then negotiates with neighboring platoon B (if existent, second responder) to perform the maneuver. Upon completion of the PLC, A sends a PLC-complete message to the EV, which then accelerates to $V_{\max}^{EV}$. Note that EV is now free to initiate another Vortex maneuver with the next downstream platoon. When A detects that the EV has passed, A initiates a PLC to move back into its original lane. The space created behind the EV is utilized, and the original vehicle configuration is preserved. If the EV chooses to continue the vortex maneuver, it will travel at $V_{\max}^{EV}$ until another front platoon is detected, and

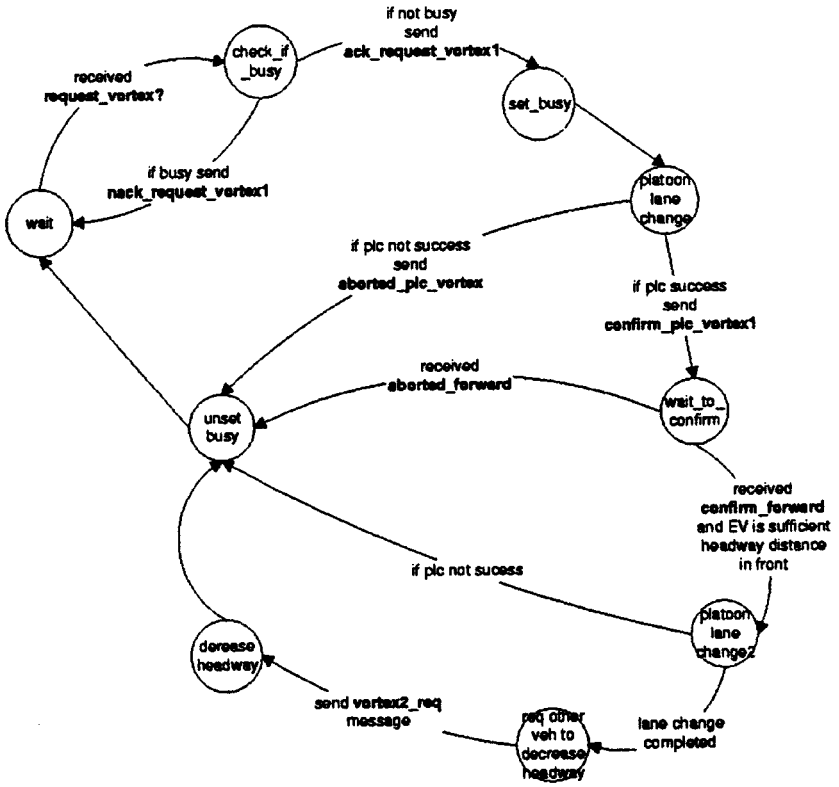

Fig. 4. Vortex responder's (A) FSM.

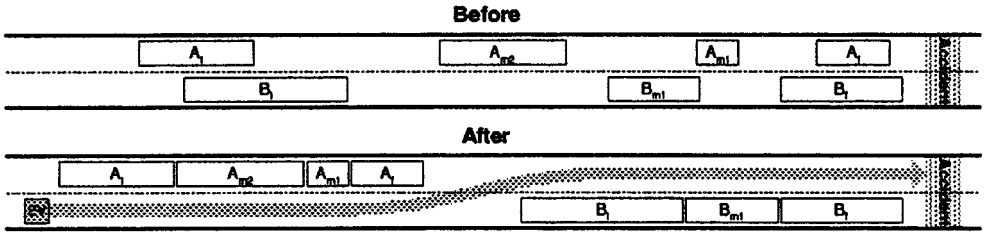

Fig. 5. Part-and-Go maneuver.

the vortex maneuver recycles. Note that platoon A changes lane so that the EV can acquire headway for faster travel. Both vehicle density and configuration are preserved. The finite-state machines (FSM) for the initiator (EV) and responder (A) are shown in Figs. 3 and 4.

B. Part-and-Go Maneuver

The part-and-go maneuver is designed to bring the EV (e.g., tow truck) to an accident site through a stagnant AHS for service (i.e., remove the debris or tow away the stopped vehicle). Note that the scenario considers that both lanes of the AHS are stopped; maneuvers for single-lane faults are ongoing work. Because vehicles are completely stopped on the AHS, backward vehicle motion is necessary for this maneuver. The part-and-go maneuver creates travel spacing for the EV by merging in sequence all platoons on both AHS lanes, and eliminating all interplatoon distances. The resulting space is used for travel headway. Fig. 5 depicts the operation of this maneuver.

Once the maneuver is initiated, the first platoon A_f on the left lane begins to backup and joins with its rear platoon, while the last platoon B_l on the right moves forward and joins with its front platoon. The required supporting maneuvers are the stationary-forward join and stationary-backward join, which are not described in detail in this paper. When a join is complete, the two platoons (e.g., A_f and A_{m1}) update themselves via radio communications to form one logical platoon. The process continues until only a single platoon is left on each lane at opposite ends of the AHS link. As a result, headway is created for the EV to travel, as conveyed by Fig. 5.

Although this maneuver is mainly controlled by the coordination layer, it is initiated and supervised by the link layer, which possesses the traffic information (i.e., total vehicle lengths and total interplatoon distances) that is essential in determining the feasibility of this maneuver.

The part-and-go maneuver will work only if the resulting gap g is large enough for the EV to change from one lane to the other. Relevant quantities in Fig. 6 are defined as follows. L_{vi} is the total vehicle length on lane i including intraplatoon dis-

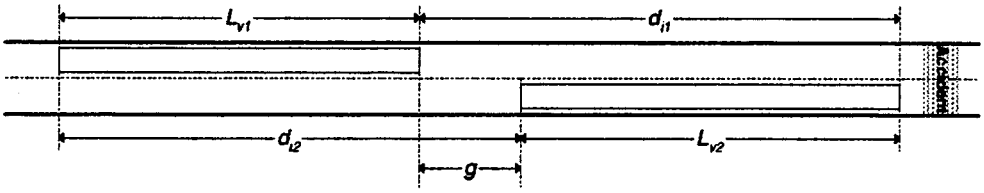

Fig. 6. Highway variable definitions.

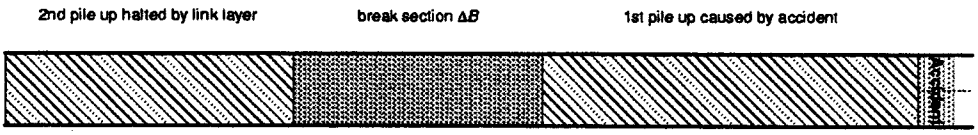

Fig. 7. Creating a break section.

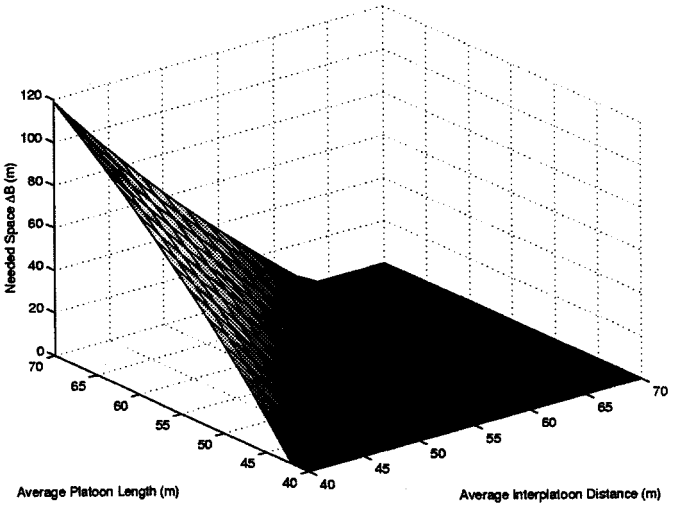

Fig. 8. Needed space ΔB for part-and-go maneuver.

tances. d_{Ii} is the total interplatoon distance on lane i. For safety purposes, g is required to be at least twice the total EV length L_{ev} [see (1)]

$$\frac{d_{I1} + d_{I2} - L_{v1} - L_{v2}}{4} \geq L_{ev}. \tag{1}$$

However, if $g < L_{ev}$, the final A platoon (after all the merges are completed) can move backward further to increase g until relation (1) holds true, assuming this rear space cushion exists. This required space can be actively created by the link layer by creating a break (ΔB) between the upstream traffic and the piled-up vehicles (Fig. 7).

The needed ΔB can be calculated as follows:

$$\Delta B = L_{ev} + \frac{N\,(L_p - L_i) - L_i}{2} \tag{2}$$

where L_p equals average platoon length, L_i equals average interplatoon spacing, and N equals average number of platoons on the AHS section.

Assuming a section length of 1000 m and an EV length of 8 m, Fig. 8 illustrates the requirement for break section length.

From Fig. 8, it can been seen that a highway populated by platoons of seven vehicles (50 m long) with platoon headways greater than 60 m does not require a break section for an EV to use the part-and-go maneuver. Similarly, a highway with shorter platoons of length 40 m will not require a break section if each platoon has a headway greater than 40 m. The FSMs for the link-layer initiator and the responders for the backward moving lane on the left (A_i) can be found in [16]. Note that the FSMs for the right-lane responders, which move forward, are almost identical to those of the left lane.

C. Zig-Zag Maneuver

The zig-zag maneuver is an alternative action in the event that there is insufficient space for the part-and-go maneuver. It has a less stringent applicability criterion; the initial available space must be *at least* the sum of the EV's length, the EV's headway tolerance distance (e.g., length of the EV) and the length of the *longest* vehicle on the highway (see Fig. 9). This criterion guarantees that the EV has sufficient headway (minimum one vehicle) for travel and space for changing lanes without consideration of individual vehicle lengths.

The EV starts the zig-zag maneuver on the shorter pile-up lane. Its initial available space is the distance from the end of the longer pile-up lane to the beginning of the downstream pile-up. This is not a restrictive criterion because stationary-forward-join maneuvers can be performed to create the initial space. Because this small initial space almost always exists due to existing interplatoon distances, the zig-zag maneuver can be applied under most circumstances.

The physical operation of the zig-zag maneuver is illustrated in Fig. 10. As the maneuver begins, the EV establishes a communications link with the leader of the adjacent platoon (L1) and determines if the initial available space criterion is satisfied. If there is no initial available space, L1 is requested to provide it by performing a stationary-forward-join maneuver. Once the space requirement is met, L1 decides which of its followers (F1) or itself will be the responder in the maneuver. This responder is determined as the *farthest* vehicle ahead that is within the EV tolerance distance (Fig. 9).

The chosen responder and its followers perform a stationary-backward join to make space for the EV. The EV can subsequently change lane and accelerate forward until a vehicle is detected ahead, at which time the EV stops within the tolerance distance. The EV then checks its lateral sensors, performs the

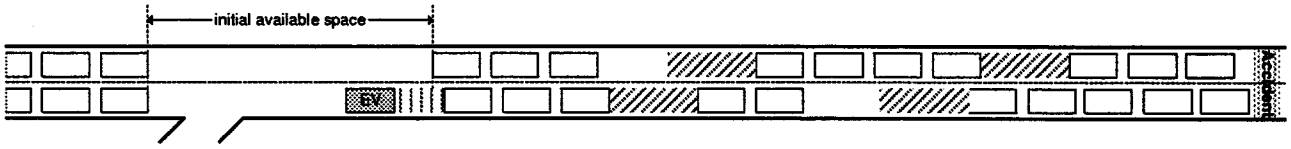

Fig. 9. Zig-zag initial available space.

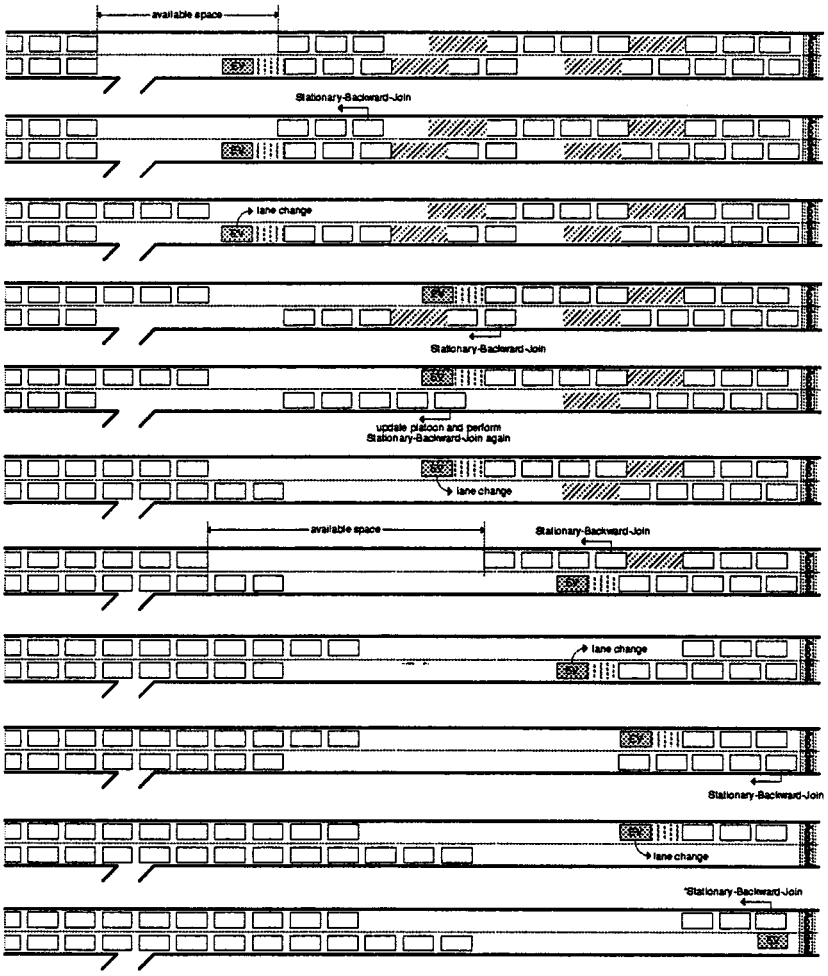

Fig. 10. Zig-zag maneuver.

lane change (if no adjacent platoon exists), and continues forward. In the event that an adjacent platoon is present, the EV will negotiate another zig-zag maneuver. This cyclic procedure continues until the EV arrives at the incident site.

The available space increases via accumulation of interplatoon distances. Consequently, the number of vehicles from a platoon which can be moved backward increases with each step. The verified FSMs for the zig-zag maneuver can be found in [16]. The time required to move each group of vehicles backwards combined with the EV's travel results in significant time for each step of the zig-zag maneuver. Compared with the part-and-go, the zig-zag is much less efficient and requires more time in bringing the EV to the accident through stopped traffic; however, it is applicable to the broadest set of traffic cases, comparatively.

D. Simulation Results

Simulation results are presented to illustrate the operation of the vortex maneuver in conjunction with the lower hierarchical control layers. The *vortex* maneuver was evaluated using SmartAHS, a traffic microsimulator [17]. SmartAHS is written in the SHIFT language [18], which is specifically designed for straightforward coding of hybrid automata. SmartAHS simulates the continuous dynamics of individual vehicles and provides a framework for defining highway topologies. California PATH projects MOU-310 and MOU-383 have produced

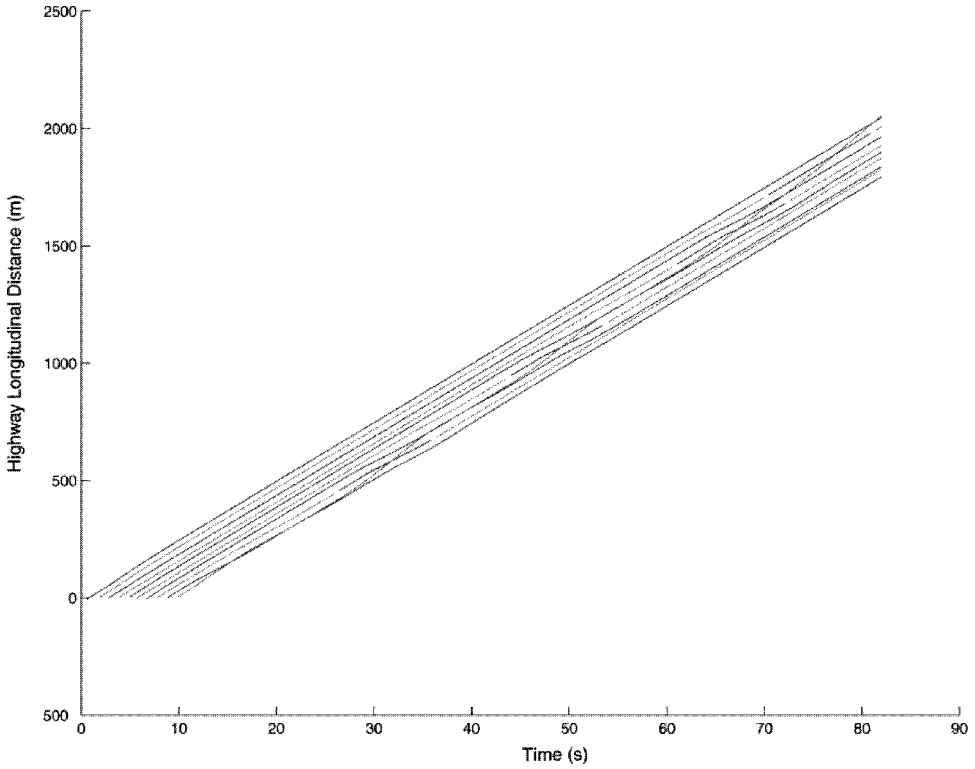

Fig. 11. TS diagram for the SmartAHS simulation of the vortex maneuver.

Smart AHS code to simulate PATH's regulation, coordination and link layer controllers. Only the normal regulation- and coordination-layer controllers were used for these simulations; the link layer was disabled.[1]

In this simulation nine vehicles and one EV are placed on a two lane AHS. The EV is the vehicle farthest upstream and must move through the group of vehicles. The simulation probably best represents the real-life scenario where an EV has to move through a cluster of vehicles on a medium-density highway before encountering the next cluster some distance downstream.

Results are shown in Fig. 11 as a time-space (TS) diagram. The implementation and testing of the *vortex* maneuver utilized only free agents. The simplified regulation-layer controllers developed as part of PATH MOU-383 are used; comfort limits on acceleration/deceleration of all vehicles are removed. The traffic flows downstream towards the right of the figure. The ten vehicles enter the two lane AHS after approximately 10 s with approximately 44 m between vehicles. The link layer speed of the non-EVs is set at 22 m/s, and that of the EV is set at 32 m/s. Each curve denotes the trajectory of a single vehicle. Dark and light denote vehicles in lanes 1 and 2, respectively. The EV is the vehicle farthest upstream, and travels in lane 2. Its trajectory has a steeper slope than any of the other vehicles. Upon receiving a vortex initiation request from the EV, the vehicle immediately downstream (*vortex* responder 1, which is denoted in light gray) decelerates to obtain safe headway space in the destination lane and forces the vehicles upstream in the target lane to also decelerate. Once there is enough space it changes lanes, which is depicted by the change of color in the vehicle's trajectory from light to dark gray. The responder returns to its original lane once the EV has passed and there is sufficient safe space.

[1]The ability to simulate enough vehicles to populate a length of AHS large enough to test several sections for the link layer is currently beyond the scope of SmartAHS. Current research associated with California PATH project MOU-383 attempts to provide large-scale highway simulation by integrating SmartCap-like mesosimulation with SmartAHS.

IV. Link Layer

To ensure that EVs have high-priority AHS transit, two design specifications for the link layer are required. First, vehicles of EV type should have higher specified velocities than other AHS vehicles. Second, a region of low vehicle density for a region around the EV is desirable from a safety standpoint. This moving region of low vehicle density is analogous to the vortex maneuver at the coordination-layer level. It is assumed that the EV moves through free-flowing traffic for this link layer maneuver. Vehicles ahead of the EV are able to make way before it comes into communication range. Because of its resemblance to a bubble in a fluid, this paper refers to the region of low vehicle density as a bubble.

A. Link Layer Flow Modeling

Traffic-low research and control has been an area of extensive research. References [19] and [20] were the first to model traffic flow as a continuum utilizing the notions of vehicle density and flow. Microscopic traffic models are produced by extrapolating the car-following behavior of human drivers to model traffic flow. Reference [21] utilized a discrete microscopic traffic-flow model with optimally determined parameters to implement real-time control of highway on-ramps. Recent traffic-flow models include [22] and [23]. On an AHS, the influence of vehicle density upon traffic flow is specified by the control

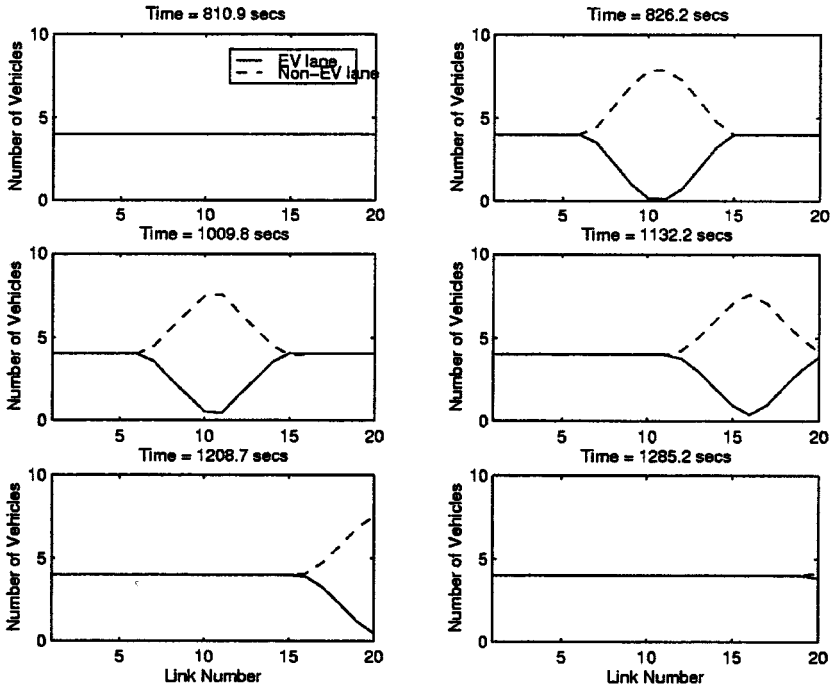

Fig. 12. Simulation 1—Vehicle densities for both lanes.

law, so that complete behavior of automated traffic is described without finding model parameters.

Link-layer flow is modeled by a set of partial differential equations based on a conservation of vehicles principle. The variables t and x refer to time and position on the highway, respectively.

- $\mathbf{K(t,\,x)} = [\mathbf{K_1(t,\,x)K_2(t,\,x)}]^{\mathbf{T}}$, vector of vehicle densities in lanes 1 and 2;
- $\mathbf{V(t,\,x)} = \mathbf{diag}\,(\mathbf{V_1(t,\,x)},\,\mathbf{V_2(t\,x)})$, diagonal matrix of vehicle velocities in lanes 1 and 2;
- $$\mathbf{N(t,\,x)} = \begin{bmatrix} -n_{1,2}(t,\,x) & n_{2,1}(t,\,x) \\ n_{1,2}(t,\,x) & -n_{2,1}(t,\,x) \end{bmatrix}$$

  where $n_{1,2}(t,\,x)$ is the proportion of vehicles per unit of time that is changing from lane 1 to lane 2 and $n_{2,1}(t,\,x)$ is the proportion of vehicles per unit time changing from lane 2 to lane 1. These proportions apply only to vehicles at position x.

The conservation of vehicles principle is expressed as

$$\mathbf{K_t} = -\,[\mathbf{VK}]_{\mathbf{x}} + \mathbf{NK}. \tag{3}$$

Subscripts t and x denote partial derivatives with respect to those variables. Spatial and time dependencies are implicit unless noted. In this modeling framework, it is possible to distinguish between vehicles traveling in different lanes. Physical highway constraints impose certain conditions on the variables involved: namely $V_i(t,\,x) \geq 0$ and $N_{i,\,j}(t,\,x) \geq 0$ for all lanes $i,\,j,\,i \neq j$. Reference [24] has also utilized (3) to study multilane traffic flow with the restrictions of time-dependent traffic speeds and lane-change proportions. In [7], a link-layer stabilizing controller [see (4)] is introduced

$$\begin{aligned} \mathbf{V} &= \mathbf{V_{des}}(x) + \mathbf{V_f} \\ \mathbf{V_f} &= \gamma(t,\,x)\mathrm{diag}\left\{\left[\mathbf{V_{des}}(x)\widetilde{\mathbf{K}}\right]_x\right\} \\ \mathbf{N} &= \mathbf{N_{des}} + \mathbf{N_f}. \end{aligned} \tag{4}$$

The controller requires specification of a desired traffic-flow behavior, in terms of $\mathbf{K_{des}}$, $\mathbf{V_{des}}$, and $\mathbf{N_{des}}$. The desired behavior must also obey the conservation of vehicles equation in order to be physically realizable. The vehicle density error is defined to be $\widetilde{\mathbf{K}} = \mathbf{K_{des}} - \mathbf{K}$. The elements of $\mathbf{N}_f$ have the same sign convention as $\mathbf{N}$ and are defined to be zero except for the following case. Let $i,\,j,\,i \neq j$ be subscripts denoting lanes 1 and 2. Equation (5) applies for the elements of $\mathbf{N_f}$

$$n_{f,i} = \max\left(0,\,\zeta_i(t,\,x)\left[\widetilde{K}_i V_{des,\,i} - \widetilde{K}_j V_{des,\,j}\right]\right). \tag{5}$$

The controller allows for desired lane-change proportions and velocities to be achieved. In [25], the expressions for feedback terms $\mathbf{V_f}$ and $\mathbf{N_f}$ in (4) are shown to guarantee convergence of the link-layer controller. The associated gains $\gamma(t,\,x)$ and $\zeta(t,\,x)$ are chosen to be positive everywhere except at the boundaries, where no control can be exerted. It is important to note that while the desired velocity field does not vary in time, the desired lane change profile may be specified as a function of time. The design of the *bubble* maneuver exploits this property.

Creation of the *bubble* maneuver is achieved by specification of a time varying $\mathbf{N_{des}}$. Assume that the EV travels in lane 2. A rate of lane change can be specified such that vehicles other than the EV in lane 2 are removed and placed in lane 1 to make way for the EV. Moreover, the excess of cars in lane 1 are returned

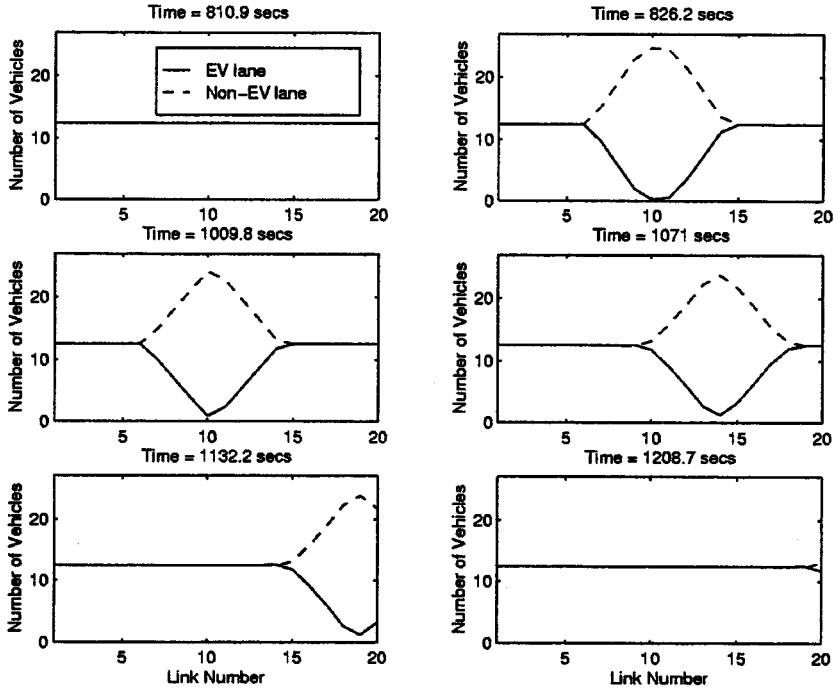

Fig. 13. Simulation 2—vehicle densities for both lanes.

to lane 2 after the faster-moving EV has passed. To achieve this *bubble* profile, the desired rates of lane change obey

$$\begin{aligned} n_{d,2,1}(t, x_e) &> 0, \quad \text{all non-EVs} \\ n_{d,2,1}(t, x_e) &= 0, \quad \text{EV} \\ n_{d,1,2}(t, x_e) &= 0, \quad \text{all non-EVs} \\ n_{d,1,2}(t, x_e) &> 0, \quad \text{EV} \end{aligned}$$

where x_e is the location of the EV at time t. These restrictions on the rates of lane change force the EV to occupy lane 2. The low-density bubble is extended spatially around the EV so that the desired proportions of lane change N_{des} vary smoothly in space and time.

B. Simulation Results

Simulation results obtained with SmartCap [26], a mesoscopic traffic-flow simulation package, of a hypothetical EV circulating on a two-lane highway are presented. SmartCap is a C program which evaluates traffic management plans for user-defined highway geometries. A traffic management plan consists of: 1) traffic velocities for different locations along the highway; 2) spacing required for maneuvers such as cruising or lane change; 3) permitted exit flows; and 4) desired entry flows. SmartCap integrates the specified traffic management plan starting at the different highway exits. Entrance flows are automatically adjusted so that a user-defined highway spacing policy is not violated. SmartCap discretizes the highway into sections. Within a section, one or more lanes are contained in parallel.

In these simulations, all vehicles are assumed independent (i.e., no platoons). All highway sections are 500 m long. A conservative safety policy which imposes constraints on vehicle spacing depending on activity and vehicle speed is assumed. For example, a vehicle cruising at 20 m/s requires approximately 23 m of headway space. Activities such as changing lane require additional space in both the originating and destination lane. In these simulations, the low-density bubble extends over seven sections of the highway. This length is more a result of the highway discretization adopted than of the control method itself.

In the first simulation, all vehicles are cruising at 20 m/s at a steady flow before the EV enters the highway. Capacity conditions so that it is possible to place all vehicles in a single lane at the same speed without violating safety conditions are assumed. Fig. 12 depicts the results. The results are expressed in number of vehicles per section. In the first plot, the vehicle densities in both lanes are the same. At $t = 800$ s, a *static* low-density bubble is created around section 10. The creation of the low-density bubble is achieved in one sampling period, approximately 15 s. Even after the entry of the EV onto the AHS, all vehicles continue to cruise at 20 m/s. In section 10, the density in lane 2 drops to zero while the density in lane 1 doubles, reflecting movement of all non-EVs into lane 1. The bubble begins to move at $t = 1000$ s with a velocity of 25 m/s. At $t = 1280$ s, the bubble has left the highway, and at $t = 1400$ s, traffic conditions are fully recovered. During the EV maneuver, the desired velocity of all non-EVs remains 20 m/s. The low-density bubble travels along the highway at a velocity of 25 m/s, allowing the EV inside to travel at faster speeds than the rest of the traffic.

The second set of results is obtained for more rigorous traffic conditions (Fig. 13). Prior to the entry of the EV, all vehicles cruise at a speed of 20 m/s. Under the imposed vehicle spacing policy for safety, a maximum of ten vehicles cruising at 20 m/s may occupy each lane of a 500 m section of highway such that they may all be accommodated in a single lane for circulation of the EV. For this example, an initial inlet flow of 1800 (vehicles/hr) is chosen for each of the two lanes to illustrate the

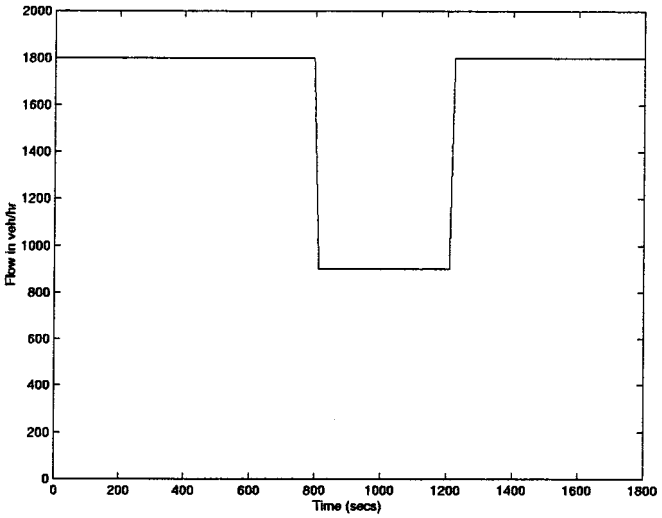

Fig. 14. Simulation 2—AHS inlet flow in each lane.

case where one lane cannot accommodate all vehicles due to space and safety constraints. At $t = 800$ s, a *static* low-density bubble is created. Immediately, inlet traffic flow must be restricted (see Fig. 14) to permit other vehicles to change lane from lane 2 into lane 1. The velocity of non EVs is also decreased to 10 m/s so that less safety spacing is needed for each vehicle. At $t = 1000$ s, the low vehicle density bubble begins to move at a velocity of 30 m/s. Traffic conditions are recovered more quickly than the first simulation. Inlet flow is again unrestricted at $t = 1200$ s. Higher inlet flows may also be accommodated by this strategy. The restriction of inlet flow would be of the same magnitude and duration as illustrated in this simulation.

These simulation results indicate that an EV can travel faster than other AHS vehicles under the illustrated circumstances. The size of the low-density bubble can be controlled to allow non-EVs more time to change lane. The opportunity to change lane is dependent upon the availability of space in the destination lane, but can also be provided by acceleration/deceleration of neighboring vehicles which requires time. Increasing vehicle density on the AHS would require the low-density bubble to extend over more links. The tradeoff associated with a larger bubble is a longer recovery time for nominal traffic conditions.

V. Conclusion

Circulation of the EV requires cooperation of both coordination and link layers. The link-layer bubble maneuver serves to circulate the majority of vehicles out of the way of the EV in free-flowing traffic. In the event that an individual vehicle or platoon is unable to respond to the commands of the link layer control, the vortex maneuver described in this paper is utilized to move the remaining vehicles out the EV's way. The other coordination-layer maneuvers, the zig-zag and part-and-go, also require assistance from the link layer in stopped traffic scenarios. Future work will include link-layer control design for traffic pileup management.

This paper describes AHS architecture design for coordination and link layers in order to accommodate EVs. Assignment of high priority to EV transit requires development of *degraded* mode control laws as described in this paper. On-going work includes the development of additional complementary coordination and regulation-layer maneuvers. The design of link-layer control strategies that do not restrict the highway inlet flow during the EV transit in the AHS have been developed [27].

References

[1] P. Varaiya and S. E. Shladover, "Sketch of an IVHS systems architecture," Institute Transport. Studies, Univ. Calif., Berkeley, Tech. Rep. UCB-ITS-PRR-91-3, 1991.

[2] P. Varaiya, "Smart cars on smart roads: Problems of control," *IEEE Trans. Automat. Contr.*, vol. AC-38, pp. 195–207, Feb. 1993.

[3] J. Lygeros, D. N. Godbole, and M. E. Broucke, "Towards a fault tolerant AHS design, Part I: Extended architecture,", Tech. Rep. UCB-ITS-PRR-96-14.

[4] D. N. Godbole, J. Lygeros, E. Singh, A. Deshpande, and A. Lindsey, "Towards a fault tolerant AHS design, Part II: Design and verification of communication protocols,", Tech. Rep. UCB-ITS-PRR-96-15.

[5] R. Horowitz, "Automated highway systems: The smart way to go," in *Proc. 8th IFAC Symp. Transportation Systems (Plenary Presentation)*, Chania, Greece, June 1997.

[6] B. Rao and P. Varaiya, "Roadside intelligence for flow control in IVHS," PATH, Univ. Calif. Berkeley, Tech. Rep., Aug. 1993.

[7] L. Alvarez, R. Horowitz, and P. Li, "Traffic flow control in automated highway systems," *Control Eng. Practice*, vol. 7, no. 11, pp. 1071–1078, 1999.

[8] F. Eskafi, D. Khorramabadi, and P. Varaiya, "An automated highway system simulator," *Trans. Res., Part C: Emerging Technol.*, vol. 3A, no. 1, pp. 1–17, 1995.

[9] D. Godbole, F. Eskafi, E. Singh, and P. Varaiya, "Design of entry and exit maneuvers for AHS," in *Proc. American Control Conf.*, 1995, pp. 3576–3580.

[10] P. Y. Li, L. Alvarez, and R. Horowitz, "AHS safe control laws for platoon leaders," *IEEE Trans. Contr. Syst. Technol.*, vol. 5, pp. 614–628, Nov. 1997.

[11] F. Eskafi, "Modeling and simulation of the automated highway systems," Ph.D. dissertation, Dept. Elect. Eng. Computer Sci., Univ. Calif. Berkeley, 1996.

[12] A. Deshpande and P. Varaiya, "Control of discrete event systems in temporal logic," Institute of Transport. Studies, PATH, Univ. California, Berkeley, CA, Tech. Rep., UCB-PATH 94-04, 1994.

[13] Z. Har'El and R. P. Kurshan, *COSPAN User's Guide*. Murray Hill, NJ: AT&T Bell Laboratories, 1987.

[14] A. Hsu, F. Eskafi, S. Sachs, and P. Varaiya, "Protocol design for an automated highway system," *Discrete Event Dyn. Syst.*, vol. 2, no. 1, pp. 4–16, 1994.

[15] Uppaal2k. Uppaal2k. Design and Analysis of Real-Time Systems Group at Uppsala Univ. Sweden and Basic Research in Computer Science Group at Aalborg Univ. Denmark. [Online]. Available: http://www.uppaal.com

[16] C. Toy, K. Leung, L. Alvarez, and R. Horowitz, "Emergency vehicle maneuvers and control laws for automated highway systems," in *Proc. ASME Int. Mechanical Engineering Congress and Exposition*, Anaheim, CA, Nov. 1998.

[17] California PATH, Berkeley, CA. SmartAHS. [Online]. Available: www.path.berkeley.edu/smart-ahs

[18] California PATH, Berkeley, CA. Shift. [Online]. Available: www.path.berkeley.edu/shift

[19] M. J. Lighthill and G. B. Whitham, "On kinematic waves II. A theory of traffic flow on long crowded roads," in *Proc. Roy. Soc., London Series A*, vol. 229, 1955, pp. 317–345.

[20] P. I. Richards, "Shockwaves on highways," *Oper. Res.*, vol. 4, pp. 42–51, 1956.

[21] M. Papageorgiou, J. M. Blosseville, and H. Hadi-Salem, "Modeling and real-time control of traffic flow on the southern part of boulevard peripherique in Paris: Part I: Modeling and Part II: Coordinated on-ramp metering," *Transport. Res., Part A: Policy and Practice*, vol. 24A, no. 5, pp. 345–370, 1990.

[22] M. Broucke and P. Varaiya, "A theory of traffic flow in automated highway system," *Transport. Res., Part C: Emerging Technol.*, vol. 4, no. 4, pp. 181–210, 1996.

[23] C. Daganzo, "The cell transmission model: A dynamic representation of highway traffic consistent with the hydrodynamic theory," *Transport. Res., Part B: Methodological*, vol. 28B, pp. 269–287, Aug. 1994.
[24] E. N. Holland and A. W. Woods, "A continuum model for the dispersion of traffic on two-lane roads," *Transport. Res., Part B: Methodological*, vol. 31, no. 6, pp. 473–485, 1997.
[25] L. Alvarez, R. Horowitz, and P. Li, "Link layer vehicle flow controller for the PATH AHS architecture," in *Proc. IFAC World Congress*, vol. Q, San Francisco, CA, 1996, pp. 207–212.
[26] M. Broucke, P. Varaiya, M. Kourjankski, and D. Khorramabadi, "Smartcap User's Guide," Department of Electrical Engineering and Computer Science, Univ. Calif., Berkeley, CA, Tech. Rep., May 1996.
[27] C. Toy, L. Alvarez, and R. Horowitz, "A traffic flow controller for non-stationary velocity profiles on automated highways," presented at the Proc. American Control Conf., San Diego, CA, June 1999.

Charmaine Toy received the M.S. degree in biomechanical engineering from Stanford University, Stanford, CA, in 1993, the B.S. degree in bioengineering and the Ph.D. degree in mechanical engineering, both from the University of California at Berkeley, in 1992 and 2000, respectively.

Currently, she is an Automation Engineer in the fiberoptics industry.

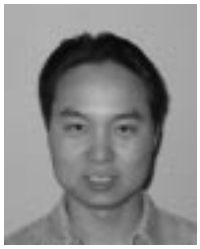

Kevin Leung received the B.S. and M.S. degrees in mechanical engineering from the University of California at Berkeley, in 1996 and 1998, respectively.

Currently, he is a Controls Engineer in the telecommunications industry.

Luis Alvarez received the Ph.D. degree in mechanical engineering from the University of California at Berkeley, in 1996.

Currently, he is a Professor of mechanical engineering at the Universidad Nacional Autónoma de México.

Roberto Horowitz (M'89–SM'02) received the B.S. and Ph.D. degrees in mechanical engineering from the University of California at Berkeley, in 1977 and 1983, respectively.

Currently, he is a Professor and the Vice-Chair of Graduate Studies in the Mechanical Engineering Department, University of California at Berkeley. His research focuses on the areas of computer mechatronics systems, microelectromechanical systems (MEMS), and intelligent vehicle and highways systems.